



A new and promiscuous α/β hydrolase from *Acinetobacter tandoii* DSM 14970^T inactivates the mycotoxin ochratoxin A

Ana Sánchez-Arroyo¹ · Laura Plaza-Vinuesa¹ · María Claudia Abeijón-Mukdsi¹ · Blanca de las Rivas¹ · José Miguel Mancheño² · Rosario Muñoz¹

Received: 17 October 2023 / Revised: 11 February 2024 / Accepted: 13 February 2024
© The Author(s) 2024

Abstract

The presence of ochratoxin A (OTA) in food and feed represents a serious concern since it raises severe health implications. Bacterial strains of the *Acinetobacter* genus hydrolyse the amide bond of OTA yielding non-toxic OT α and L- β -phenylalanine; in particular, the carboxypeptidase PJ15_1540 from *Acinetobacter* sp. *neg1* has been identified as an OTA-degrading enzyme. Here, we describe the ability to transform OTA of cell-free protein extracts from *Acinetobacter tandoii* DSM 14970^T, a strain isolated from sludge plants, and also report on the finding of a new and promiscuous α/β hydrolase (ABH), with close homologs highly distributed within the *Acinetobacter* genus. ABH from *A. tandoii* (*AtABH*) exhibited amidase activity against OTA and OTB mycotoxins, as well as against several carboxypeptidase substrates. The predicted structure of *AtABH* reveals an α/β hydrolase core composed of a parallel, six-stranded β -sheet, with a large cap domain similar to the marine esterase EprEst. Further biochemical analyses of *AtABH* reveal that it is an efficient esterase with a similar specificity profile as EprEst. Molecular docking studies rendered a consistent OTA-binding mode. We proposed a potential procedure for preparing new OTA-degrading enzymes starting from promiscuous α/β hydrolases based on our results.

Key points

- *AtABH* is a promiscuous $\alpha\beta$ hydrolase with both esterase and amidohydrolase activities
- *AtABH* hydrolyses the amide bond of ochratoxin A rendering nontoxic OT α
- Promiscuous $\alpha\beta$ hydrolases are a possible source of new OTA-degrading enzymes

Keywords Amidohydrolase · Esterase · Mycotoxin · Ochratoxin A · Promiscuous enzymes

Introduction

Ochratoxin A (OTA) is one of the most prevalent mycotoxins that contaminate food and feed products around the world (Liuzzi et al. 2017; Marin et al. 2013). OTA can have a variety of noxious effects both in humans and in other

animals (Gan et al. 2017), although it is best known for its nephrotoxic effects (Pfohl-Leskowicz and Manderville 2007). While a positive association between some mycotoxins, such as aflatoxin, and cancer has been verified (Claeys et al. 2020), the potential link between OTA exposure and cancer risk is not currently established and needs further epidemiological studies. Nonetheless, to avoid its toxic effects, the levels of OTA must be reduced as much as possible. Up to now, the most important measures to control OTA levels have focused on avoiding fungal growth and OTA production (Amézqueta et al. 2009). In this regard, biological approaches have increasingly been considered as an alternative to physical and chemical treatments (Abraham et al. 2022), and currently, it has been reported that microorganisms that adsorb and/or degrade OTA and even some practical procedures have been developed thereafter (Ndiaye et al. 2022). However, some reports describing microbial OTA-degrading activity do not discriminate between

✉ José Miguel Mancheño
jm.mancheno@csic.es

✉ Rosario Muñoz
r.munoz@csic.es

¹ Bacterial Biotechnology, Institute of Food Science, Technology and Nutrition (ICTAN), CSIC, José Antonio Novais 6, 28040 Madrid, Spain

² Department of Crystallography and Structural Biology, Institute of Physical Chemistry Blas Cabrera, CSIC, Serrano 119, 28006 Madrid, Spain

physical adsorption or enzymatic degradation. In this line, it is now generally accepted that whereas detoxification by lactic acid bacteria mainly proceeds through adsorption of OTA to their cell walls (Del Prete et al. 2007), other organisms, including actinobacteria, bacteria, filamentous fungi, and yeast (Xu et al. 2022), transform OTA through hydrolysis of its amide bond to generate OT α and L- β -phenylalanine, virtually non-toxic compounds.

Only a handful of enzymes involved in the degradation of OTA have been isolated and characterized in detail. The first reported microbial (fungal) ochratoxinase was an *Aspergillus niger* amidase (Dobritzsch et al. 2014). Later, bacterial proteins annotated as putative carboxypeptidases from *Bacillus amyloliquefaciens* ASAG1 (Chang et al. 2015), *Bacillus subtilis* CW14 (Hu et al. 2018; Xu et al. 2021), *Lysobacter* sp. CW239 (Wei et al. 2020), and *Acinetobacter* sp. *neg1* (Liuzzi et al. 2017) were described. Moreover, bacterial enzymes able to efficiently transform OTA have been identified in *Alcaligenes faecalis* DSM 16503 (Zhang et al. 2019), and *Stenotrophomonas* sp. CW117 (Chen et al. 2022; Luo et al. 2022). In this regard, we have recently reported that the salicylate 1,2-dioxygenase from *Pseudaminobacter salicylatoxidans* inactivates OTA acting as an amidohydrolase and proposed that metalocarboxypeptidases may be a rich source of potential OTA-degrading enzymes (Sánchez-Arroyo et al. 2023). In that study, with the aid of currently available, powerful molecular docking approaches, we proposed an OTA-binding mode and a catalytic mechanism of OTA hydrolysis, which is consistent with those from metalocarboxypeptidases. This very same in silico approach is being used here, combined with the use of AlphaFold2 (Jumper et al. 2021) for predicting the structure of AtABH. In this sense, the accuracy of the predicted models produced by this astonishingly powerful program (Pereira et al. 2021) is such that it has changed the scene of structural biology, and they are used for the generation of convincing hypotheses about interacting proteins (Tunyasuvunakool et al. 2021) or structure solution by molecular replacement (McCoy et al. 2022; see Read et al. 2023).

Bacteria from the genus *Acinetobacter* are widely distributed in nature, being present in soils, freshwater, oceans, sediments, and contaminated sites (Jung and Park 2015). *Acinetobacter* species are metabolically versatile in that they possess numerous catabolic routes aimed at the degradation of compounds from plants, such as routes for the degradation of various long-chain dicarboxylic acids and aromatic and hydroxylated aromatic compounds. For these reasons, the genus *Acinetobacter* has attracted significant attention both in the scientific and the biotechnological fields (Jung and Park 2015), particularly, the strains *A. calcoaceticus* NRRL B551 and *A. calcoaceticus* 396.1 since they are able to transform OTA (De Bellis et al. 2015; Hwang and Draughon 1994). However, the *Acinetobacter* genus

includes both non-pathogenic and pathogenic species; for instance, the *Acinetobacter baumannii-calcoaceticus* complex causes diverse human infections, the nosocomial ones affecting immunocompromised patients being especially relevant (Blossom and Srinivasan 2008; Zarrilli et al. 2023). Hence, it does not seem to be the most adequate bacterial species for biotechnological applications in the food industry. A comparable scenario is found for the *Acinetobacter* sp. *neg1* strain: although it is also capable of degrading OTA (De Bellis et al. 2015), shows the closest match to *A. gyllenbergii* (Fanelli et al. 2015), a haemolytic species isolated from human clinical specimens (Nemec et al. 2009) that has been described to be the origin of resistance to aminoglycosides of therapeutic importance in *Acinetobacter* strains (Yoon et al. 2016). Curiously, the recombinant variant of the carboxypeptidase PJ15_1540 from *Acinetobacter* sp. *neg1* exhibited a much lower OTA-degrading activity than that of the host strain (Liuzzi et al. 2017).

In this study, we analyzed the OTA-degrading ability of the bacterial species *A. tandoii* (Carr et al. 2003), a non-pathogenic species isolated from sludge plants, and identified a new α/β hydrolase in *A. tandoii* DSM 14970^T (AtABH) that degrades OTA by hydrolysing its amide bond, producing OT α and L- β -phenylalanine. Modelling of the structure of AtABH with AlphaFold2 and subsequent in silico molecular docking approaches permitted us to propose an OTA-binding mode to AtABH that reveals a substrate-binding pocket with two hydrophobic sub-pockets around a catalytic triad. Further structural similarity searches show unexpected relationships of AtABH with esterases, which has been verified experimentally revealing that AtABH is a promiscuous α/β hydrolase with an efficient esterase activity and a second, ancillary amidohydrolase activity. Based on these findings, we propose a structure-based roadmap for finding OTA-degrading enzymes.

Materials and methods

Bacterial strains and OTA-transformation assays

Acinetobacter tandoii DSM 14970^T type strain used in this study was purchased from the Leibniz Institute DSMZ-German Collection of Microorganisms and Cell Cultures (DSMZ) and was routinely grown in TSB broth at 30 °C as recommended by DSMZ. *Escherichia coli* DH5 α was used for DNA manipulations. *E. coli* BL21 (DE3) cells were used for protein expression in the pURI3-Cter vector (Curiel et al. 2011). *E. coli* strains were cultured in Luria–Bertani (LB) medium at 37 °C and shaking. When required, ampicillin was added to the medium at 100 μ g/mL.

A. tandoii DSM 14970^T cultures and cell-free protein extract were used to assay their ability to transform OTA.

For the bacterial culture assays, *A. tandoii* was grown in minimal salt medium (MM) (Shabtai and Gutnick 1985), ethanol-minimal salt medium (pH 7.5; 2.5% ethanol; MME) (Hwang and Draughon 1994; Shabtai and Gutnick 1985), and minimal salt medium with Bacto Peptone (0.5% w/v) (MMP) (De Bellis et al. 2015). Cultures were grown for 6 days in the absence or in the presence of OTA (5 μ M). Then, the cells were sedimented, and the supernatant was filtered (0.45 μ m pore size; Sarstedt, Germany) and analyzed by HPLC for the presence of OTA as previously described (Sánchez-Arroyo et al. 2023).

The OTA transforming activity was also analyzed in cell-free protein extract. For extract preparation, *A. tandoii* DSM 14970^T cells grown in TSB broth for 24 h were harvested by centrifugation (8000 \times g for 15 min at 4 °C), washed with 50 mM MOPS buffer, pH 7.0 containing 20 mM NaCl, and resuspended in the buffer used for cell rupture. Bacterial cells were disintegrated by using a French press at 1100 psi pressure (Amicon French pressure cell, SLM Instruments). Cell disruption steps were carried out on ice to ensure the low-temperature conditions required for most enzymes. To remove cell debris, the cell suspension was centrifuged at 4 °C (12,000 \times g for 20 min). To prepare the final protein extract, the clean supernatant was filtered with sterile filters of 0.45 μ m pore size (Sarstedt, Germany). For OTA degradation assays, this protein extract was incubated in the presence of OTA (5 μ M final concentration) overnight at 37 °C. Reactions were stopped by heating at 95 °C for 5 min. Subsequently, samples were centrifuged at 14,000 \times g for 5 min. The supernatants were filtered through 0.45 μ m syringe filters (Millipore, USA) and diluted 1:1 in water/ acetonitrile/glacial acetic acid (89:10:1, v/v), and analyzed by HPLC as previously described (Sánchez-Arroyo et al. 2023). Controls without proteins were analyzed to evaluate the spontaneous degradation of OTA. Identification of the degradation product as OT α was carried out by comparing its retention time and spectral data with those of OT α from a commercial supplier (LGC Standard, UK).

Production and purification of an α/β hydrolase from *A. tandoii*

In the *A. tandoii* DSM 14970^T genome, the gene encoding a putative α/β hydrolase in the locus Q340_RS0119210 (*AtABH*) was amplified by PCR using primers 1965 (5'-AAC TTTAAGAAGGAGATATACATatgaaaccactgatccactttgcga) and 1966 (5'-GCTATTAATGATGATGATGATGATGttgcctgaatcaactgcttaatcaa) (italics: nucleotides pairing the expression vector; lowercase letters: nucleotides pairing the gene sequence). The 795-bp purified PCR product was inserted into the pURI3-Cter vector as described previously (Curiel et al. 2011). The resultant recombinant protein variants have a six-histidine affinity tag in their C-termini. *E. coli* DH5 α

cells were used for preparing the plasmids that were then transformed into *E. coli* BL21(DE3) cells. Protein production and purification of the His-tagged AtABH was carried out essentially as described before (Sánchez-Arroyo et al. 2023). Briefly, *E. coli* cells carrying the recombinant plasmid pURI3-Cter-ABH were grown at 22 °C in LB medium and induced with 0.25 mM isopropyl- β -D-thiogalactopyranoside (IPTG) (Ackerley et al. 2004). The cell lysate obtained by disruption with a French press was centrifuged at 47,000 \times g for 40 min at 4 °C to remove the insoluble fraction. AtABH was purified by IMAC using TALON superflow resin (Clontech). The eluted His-tagged AtABH was dialyzed overnight at 4 °C against 50 mM sodium phosphate buffer, pH 7.0, containing 300 mM NaCl. The purity of the enzyme was checked by SDS-PAGE.

Enzymatic degradation of OTA, OTB, and 4MF

Degradation of the mycotoxins OTA and ochratoxin B (OTB) was followed by HPLC. Stock solutions of OTA and OTB at 1 mg/mL concentration were prepared by dissolving them in methanol and stored at -20 °C. The enzymatic hydrolysis reactions were conducted essentially as described previously, with minor modifications (Sánchez-Arroyo et al. 2023).

Conversely, we also used the OTA analog *N*-(4-methoxyphenylazoformyl)-phenylalanine (4MF) (Bachem, Switzerland) as substrate, to compare the degradation activity of purified AtABH with the commercial CPA (Sigma-Aldrich, Germany). Hydrolysis of 4MF was assayed as described (Sánchez-Arroyo et al. 2023).

AtABH activity on synthetic carboxypeptidase substrates

The specificity profile of AtABH was analyzed by using a set of synthetic carboxypeptidase substrates with different amino acid residues at their C-terminal position. We have classified the substrates tested into three different families according to their chemical composition (Fig. S1 in the Supplementary information). Family I is composed of carbobenzyloxy- β -alanyl-L-alanine (ZAA); this compound is the only substrate containing a β -amino acid. Family II is composed of six potential carbobenzyloxy-derived substrates: carbobenzyloxy-L-alanine (ZA), carbobenzyloxy-L-alanyl-L-leucine (ZAL), carbobenzyloxy-L-alanyl-L-phenylalanine (ZAF), carbobenzyloxy-L-isoleucyl-L-phenylalanine (ZIF), carbobenzyloxy-L-phenylalanine (ZF), and carbobenzyloxy-L-phenylalanyl-L-isoleucine (ZFI). As can be observed, this family contains potential substrates with one (ZA, and ZF) or two (ZAL, ZAF, ZIF, ZFI) amino acids, together with the N-terminal carbobenzyloxy moiety. Finally, family III is made up of the hippuryl-derived

compounds: hippuryl-phenylalanine (N-benzoyl-glycyl-phenylalanine) (HF), and hippuryl-arginine (N-benzoyl-glycyl-arginine) (HR). All these substrates were purchased from Sigma-Aldrich (Germany) and were manipulated as described previously (Sánchez-Arroyo, et al. 2023).

Esterase enzymatic assay

The esterase activity of *AtABH* was determined by a spectrophotometric method using *p*-nitrophenyl esters of different chain lengths (Sigma-Aldrich) as substrates: *p*-nitrophenyl acetate (C2), *p*-nitrophenyl butyrate (C4), *p*-nitrophenyl caprylate (C8), *p*-nitrophenyl laurate (C12), *p*-nitrophenyl myristate (C14), and *p*-nitrophenyl palmitate (C16), as described previously (Esteban-Torres et al. 2013). Stock solutions (25 μ M) of the *p*-nitrophenyl esters were prepared in acetonitrile-isopropanol (1/4, v/v).

The enzymatic reactions were done in 50 mM sodium phosphate buffer (pH 7.0) containing the substrate at 0.5 mM final concentration, and 30 μ g of *AtABH* (3.8 μ M). After 10 min of incubation at 37 °C, the reaction was stopped by chilling on ice, and the amount of *p*-nitrophenol released was determined as described before (Esteban-Torres et al. 2013). Enzyme assays were performed in triplicate.

Molecular docking studies

Molecular docking was performed with the docking program AutoDock Vina (Forli et al. 2016) using UCSF Chimera 1.17 (Pettersen et al. 2004) as interface. We used the predicted structure of *AtABH* with AlphaFold2 (Jumper et al. 2021) as the receptor. Before its use in docking assays, the PDB file from AlphaFold2 was processed with Phenix (Liebschner et al. 2019), first with *phenix.process_predicted_model*, and then with *phenix.geometry_minimization*. The final, minimized model of *AtABH* was checked with Molprobit (Williams et al. 2018) and it showed excellent stereochemistry. In this regard, as expected for a canonical nucleophile serine residue of α/β hydrolases such as *AtABH*, its predicted catalytic serine residue (Ser75) is an outlier in the Ramachandran plot (there are 3 outliers out of 262 amino acids). The other two outlier residues are Pro35 and Phe225, which are far from the active site of *AtABH* and therefore are not relevant in the docking assays. On the other hand, the atomic coordinates of OTA (PubChem CID: 442,530) and OTB (PubChem CID: 20,966) were taken from the PubChem database (<https://pubchem.ncbi.nlm.nih.gov/>). The atomic coordinates for the OTA homolog 4MF were prepared with Chimera (Pettersen et al. 2004) by modifying those of OTA. The preparation of the structure of the receptor for docking assays involved the addition of polar hydrogens and the merging of the charges, and the preparation of the ligand involved the addition of hydrogens and Gasteiger

charges. Additional parameters were: search exhaustiveness of 8, a maximum energy difference of 3 kcal/mol, and the number of binding modes was 10. The molecular docking was done using a grid box search space with dimensions $x=15$ Å, $y=15$ Å, and $z=15$ Å centered at the coordinates of the oxygen atom of the Ser75 side chain. Evaluation of the best-docked poses was carried out considering that the scissile amide bond must be in close proximity and in the correct orientation to the nucleophile Ser75 side chain. UCSF Chimera (Pettersen et al. 2004), COOT (Emsley et al. 2010), and PyMOL (Schrödinger and DeLano 2020) were used for the visualization of the structures, analysis of the interactions, and figure preparation.

Prediction of the structure of the carboxypeptidase PJ15_1540 from *Acinetobacter* sp. *neg1* was also done with AlphaFold2 (Jumper et al. 2021). The resultant PDB file was processed with Phenix (Liebschner et al. 2019) as described above for *AtABH*. Structural similarity searches were done with the DALI Protein Structure Comparison Server (Holm 2022) (<http://ekhidna2.biocenter.helsinki.fi/dali/>). Pairwise structural superpositions were done with FATCAT (Li et al. 2020). Analyses of protein sequences for the presence of signal peptides were done with SignalP—6.0 (Almagro Armenteros et al. 2019) (<https://services.healthtech.dtu.dk/services/SignalP-6.0/>).

Results

Ochratoxin transformation by *A. tandoii* DSM 14970^T

We observe that *A. tandoii* DSM 14970^T was unable to grow in minimal-salts media devoid of carbon source, even in the presence of OTA. However, evident growth was detected when it was cultured in minimal media containing ethanol or peptone, regardless of the presence of OTA. Supernatants from these OTA-containing cultures were analyzed by HPLC for the presence of this mycotoxin. Although a slight reduction in OTA concentration with respect to controls was observed, the majority of OTA remained untransformed in the culture supernatant (data not shown), so it cannot be ruled out that the reduction observed could be due to degradation or a phenomenon of OTA adsorption to the bacterial cell walls.

Since the results obtained with bacterial cultures from *A. tandoii* DSM 14970^T were not conclusive, OTA degradation was assayed in a cell-free protein extract. As shown in Fig. 1, when protein extract from this strain was assayed, the OTA present in the reaction was hydrolysed, and the presence of OT α was detected in the *A. tandoii* protein extract reaction (Fig. 1). This result confirmed that *A. tandoii* DSM 14970^T hydrolyses the amide bond of OTA, producing the innocuous products OT α and L- β -phenylalanine.

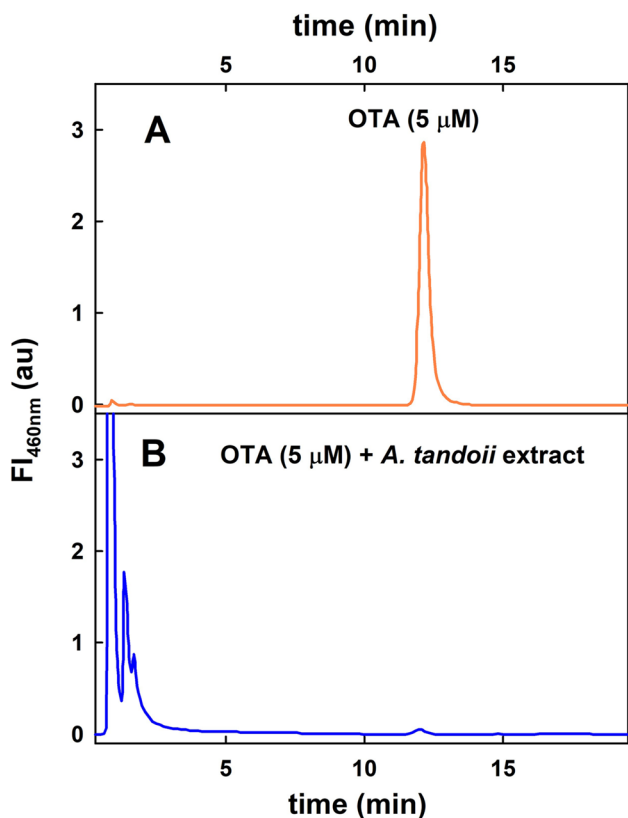


Fig. 1 Amidase activity of *A. tandoii* DSM 14970^T cell-free protein extract on OTA. HPLC chromatograms of *A. tandoii* extract incubated at 37 °C for 16 h in the presence of OTA (5 μM). A control reaction without extract is indicated (A). The fluorescence wavelengths were 340 nm for excitation and 436 nm for emission

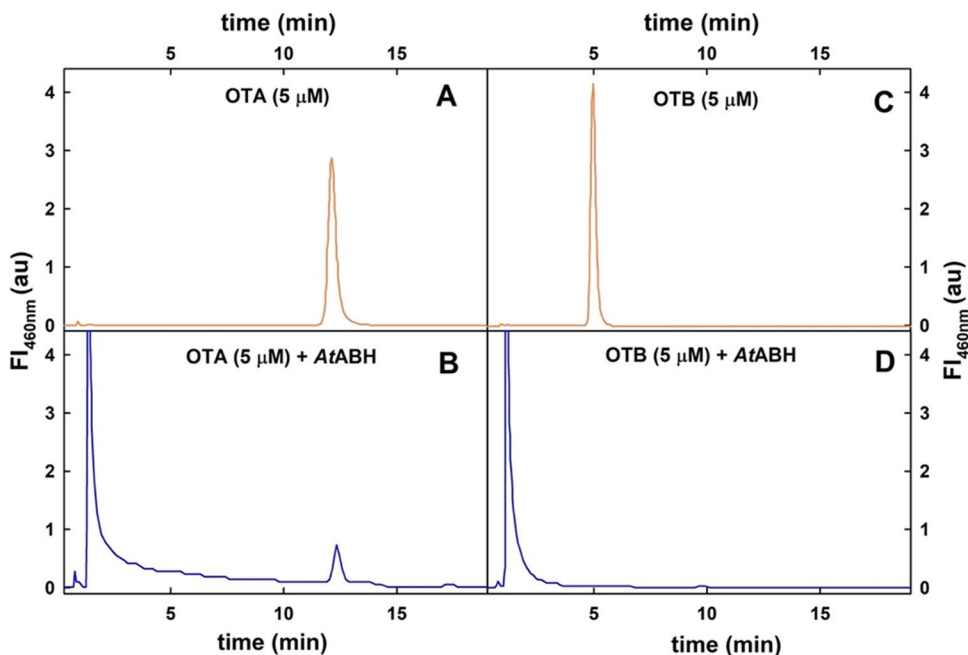
OTA-hydrolyzing activity of an α/β hydrolase from *A. tandoii*

With the aim to identify putative OTA-degrading enzymes from *A. tandoii* DSM 14970^T, we performed a protein search in the *A. tandoii* DSM 14970^T genome. In particular, we focused our attention on genes coding for hydrolases or lactamases since they have been predicted as good OTA-degrading candidates (Xu et al. 2021). From the proteins annotated as hydrolases in the *A. tandoii* DSM 14970^T genome, the “α/β hydrolase” encoded in the locus Q340_RS0119210 (WP_026441294), herein referred as *AtABH*, was chosen to check its OTA-transforming activity because it is widely distributed in *Acinetobacter* species, including the *Acinetobacter* sp. *neg1* strain (locus PJ15_RS15480, WP_047432341) (Fig. S2 in the Supplementary information).

Hence, the gene encoding *AtABH* was cloned into the pURI3-Cter vector as described previously (Curiel et al. 2011). The C-terminally His-tagged *AtABH* protein thus produced was purified by IMAC chromatography. Fig. S3 in the Supplementary information shows that the band of purified *AtABH* in SDS-PAGE corresponded to the molecular size expected for the enzyme (≈30 kDa). This final production yield was 6.9 mg of *AtABH* per liter of culture.

Pure *AtABH* was incubated overnight in the presence of OTA or OTB (a nonchlorinated form of OTA), and then the reaction mixtures were analyzed by DAD-FL-HPLC. As shown in Fig. 2, both mycotoxins were hydrolysed, yielding the expected products. In particular, the molecular species with a retention time of 1.4 min (Fig. 2B) was identified as OTα since both the retention time and its spectral properties

Fig. 2 Amidase activity of ABH from *A. tandoii* DSM 14970^T on OTA (A) and OTB (B). HPLC chromatograms of *AtABH* incubated at 37 °C for 16 h in the presence of OTA (B) and OTB (D) at 5 μM concentration. Control reactions without *AtABH* are indicated (A and C). The fluorescence wavelengths were 340 nm for excitation and 436 nm for emission



are identical to those from the commercial standard. Therefore, *AtABH* behaves as an amidohydrolase since it hydrolysed OTA producing OT α and L- β -phenylalanine.

Analysis of the specificity profile of *AtABH*

To explore the hydrolase specificity profile of *AtABH*, we used three structural families of substrates (Fig. S1 in the Supplementary information), which permitted us to probe the effects on the hydrolase activity of different substituents at both the N- and the C-terminal sides around the scissile amide bond. In this regard, since OTA, OTB, as well as the OTA analog *N*-(4-methoxyphenylazofornyl)-phenylalanine 4MF (not shown) are hydrolysed by *AtABH* and all of them contain a phenylalanyl moiety at their C-terminal end and an aromatic ring at the N-terminal end, it is expected that *AtABH* exhibited a preference for hydrophobic moieties at both the N- and C-terminal sides of the amide bond, a fact that is well supported by our modelling studies about the OTA-binding mode to *AtABH* (see below). The results obtained with the family composed of the substrates HF and HR (Fig. 3) agree well with this hypothesis since the presence in HR of a large, cationic moiety at the C-terminal side of the amide bond makes this compound a poorly hydrolysed substrate (3%) when compared to HF that presents a Phe residue (74%). Nonetheless, the presence of aromatic rings at both ends of the structure of a (putative) substrate is not a necessary condition for efficient hydrolysis as can be deduced from ZAA (100%) that contains only one aromatic ring at the N-terminal end, a C-terminal methyl group and a

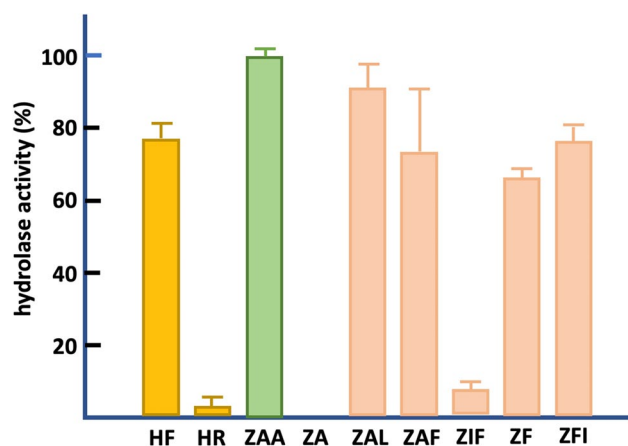


Fig. 3 Substrate profile of *A. tandoii* ABH amidase activity on carboxypeptidase synthetic substrates harbouring different substitutions around the scissile amide bond. The substrates are HF, HR, ZAA, ZA, ZAL, ZAF, ZF, ZIF, and ZFI (see Fig. S1 in the Supplementary information for structural details). The error bars represent the standard deviation estimated from the three independent assays. The observed maximum activity was defined as 100%. Colour code is as in Fig. S1

β -alanyl bridge in the central part of the molecule (Fig. S1 in the Supplementary information). Yet, the combined absence of a central bridge and a C-terminal Phe, as in ZA, was crucial for hydrolysis since this compound was not hydrolysed (Fig. 3). Since all the rest of the compounds from the ZA family were efficiently hydrolysed (excluding ZIF, which has a rigid Ile residue within the central bridge), it can be deduced that, for members of this family, the presence of both a central bridge and a C-terminal aromatic/aliphatic residue are sufficient conditions to define a good substrate for *AtABH*. As indicated below, these results are in agreement with the *in silico* model of the structure of *AtABH* that predicts a substrate-binding pocket composed of two hydrophobic sub-pockets around its canonical catalytic triad.

In silico structural model of *AtABH*

In agreement with the genomic annotation of the locus Q340_RS0119210 from *A. tandoii* DSM 14970^T, the predicted structure of *AtABH* obtained with AlphaFold2 (Jumper et al. 2021) indicates that this enzyme belongs to the α/β hydrolase superfamily of enzymes (Heikinheimo et al. 1999; Nardini and Dijkstra 1999; Ollis et al. 1992). The predicted structure of *AtABH* indicates that when compared to the canonical α/β hydrolase fold, whose core structure is based on an eight-stranded mostly parallel β -sheet, *AtABH* lacks the first two, N-terminal canonical β -strands, and therefore its structural core is a parallel, six-stranded β -sheet (Fig. 4a). The catalytic machinery of *AtABH* supported by this structural framework, as it is typical in the α/β hydrolases (Rauwerdink and Kazlauskas 2015), is based on a catalytic triad made up of residues Ser75, Asp99, and His244 (Fig. 4b). The nucleophile Ser75 is situated in a Gly-Xxx-Ser-Xxx-Gly canonical sequence motif (73-Gly-His-Ser-Leu-Gly-77), which is predicted to adopt a sharp turn, known as nucleophile elbow, between strand β 3 and helix α 3. Conversely, His244 and Asp99 are located in the β 9- α 12 and the β 4- α 4 connecting loops, respectively. The large insertion between the β 4 and β 5 strands forming the cap domain of *AtABH* is made up of the segment between residues Asp99 and Pro209 that, as shown in Fig. 4a, configures the walls of the substrate binding pocket of the enzyme.

OTA-binding mode

Following the same experimental procedure that we have recently used for the analysis of the OTA-binding mode to the salicylate 1,2-dioxygenase from *Pseudaminobacter salicylatoxidans* (Sánchez-Arroyo et al. 2023), we analyzed the binding mode of OTA, OTB, and 4MF to the predicted structure of *AtABH*. The grid box search space was centred around the residue Ser75, whose identification as the nucleophile was straightforward since, as indicated

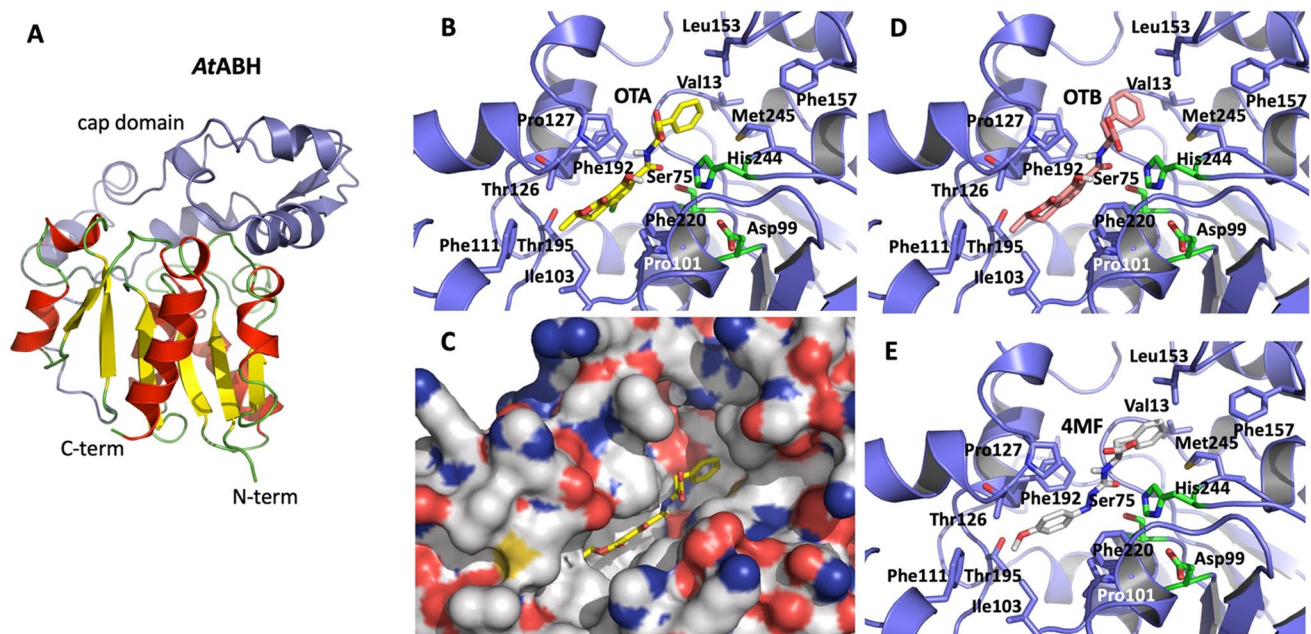


Fig. 4 Predicted model of the structure of *AtABH* with AlphaFold2 and in silico molecular docking of ochratoxin A OTA, OTB, and 4MF (see Fig. S1 in the Supplementary information for structural details). The structure of *AtABH* (A) shows an $\alpha\beta$ hydrolase fold formed by a parallel, six-stranded β -sheet (β -strands in yellow) surrounded by α -helices (in red) with a large cap domain (blue ribbon). The cap domain is comprised of the segment between residues Asp99 and Pro209 and is shown as blue ribbon. The OTA-binding mode (B, C) reveals that its amide bond is situated in close proximity to the

nucleophile Ser75 that together with Asp99 and His244 made up the catalytic triad of *AtABH* (green sticks). The substrate-binding pocket is formed by a crevice (C) which has two hydrophobic sub-pockets around the nucleophile Ser75, where the two ends of the substrates bind. OTB (D) and 4MF (E) binding modes are almost identical to the one of OTA (B). Amino acid side chains that form the substrate-binding pocket are shown as blue sticks model. OTA, OTB, and 4MF are shown as yellow, orange, and grey sticks, respectively

above, a catalytic triad defines the catalytic machinery of $\alpha\beta$ hydrolases (Fig. 4b). The catalytic triad residues of *AtABH* (Ser75, Asp99, and His244) are situated at the bottom of a crevice (Fig. 4c) where the three substrates get access. The combined analysis of the docked poses of these three substrates permitted us to infer a consistent substrate-binding mode that places their corresponding scissile amide bonds in close proximity to the Ser75 side chain. As expected, the binding of OTA (Fig. 4b and c) and OTB (Fig. 4d) is almost identical: the (3R)-5-chloro-8-hydroxy-3-methyl-1-oxo-3,4-dihydroisochromene moiety of OTA (OTB lacks the 5-chloro substituent) is sandwiched between the side chains of the two pairs of residues Pro127, Phe192, and Pro101, Phe220, respectively, and it reaches a sub-pocket formed by the side chains of Ile103, Phe111, Thr126, and Thr195. On the other hand, the aromatic ring of the Phe residue of OTA (or OTB) occupies another sub-pocket where it interacts with the Val13, Leu153, and Met245 side chains. Finally, the binding of 4MF places its amide bond in the same position and orientation observed for OTA or OTB, and its two aromatic rings occupy the two sub-pockets indicated above (Fig. 4e). The carboxylate moiety occupies the same location in all three cases and protrudes toward the solvent.

Structural similarity searches

Once an OTA-binding mode compatible with the predicted structure of *AtABH* has been determined, we carried out structural similarity searches using the DALI server (Holm 2022) with the aim of finding other potential OTA-hydrolysing enzymes, structurally similar to *AtABH*. The results show that the hits with the highest Z-score values (see Table 1) not only presented the conserved $\alpha\beta$ hydrolase fold but also very similar cap domains (Fig. 5).

Esterase activity in *AtABH*

Based on the structural similarity found between *AtABH* and the marine esterase EprEst (Zhu et al. 2021) (PDB entry: 7c4d; see Table 1) and also in the fact that many $\alpha\beta$ hydrolases have multiple catalytic activities (Bauer et al. 2020), we consider the potential esterase activity of *AtABH* using different *p*-nitrophenyl (*p*NP) esters of various acyl chain lengths (C2 to C16) as substrates. Substrate specificity was assayed after a 10-min incubation at 37 °C. Our results indicate that *AtABH* hydrolysed water-soluble *p*-NP esters, with a marked preference for the shortest substrates C2 > C4 > > C8 (Fig. 6), and remarkably, also *p*-NP

Table 1 Structurally similar proteins to *AtABH* determined with DALI

Protein	Z-score	rmsd (Å)	lali ¹	%id ²	Catalytic triad residues	Cap domain
<i>AtABH</i>	–	–	–	–	Ser75/His244/Asp99	Asp99-Pro209
2y6v	20.6	2.8	242	17	Ser145/His323/Glu169	Glu169-Arg284
7dbl	20.1	2.8	242	22	Ser139/His365/Asp163	Asp163-Arg315
7c4d	19.4	3.1	230	13	Ser85/His242/Asp109	Asp109-Pro205
1m33	19.1	2.7	210	14	Ser82/His235/Asp207	Ala106-Pro198

¹lali, number of aligned residues; ²%id, sequence identity to *AtABH*

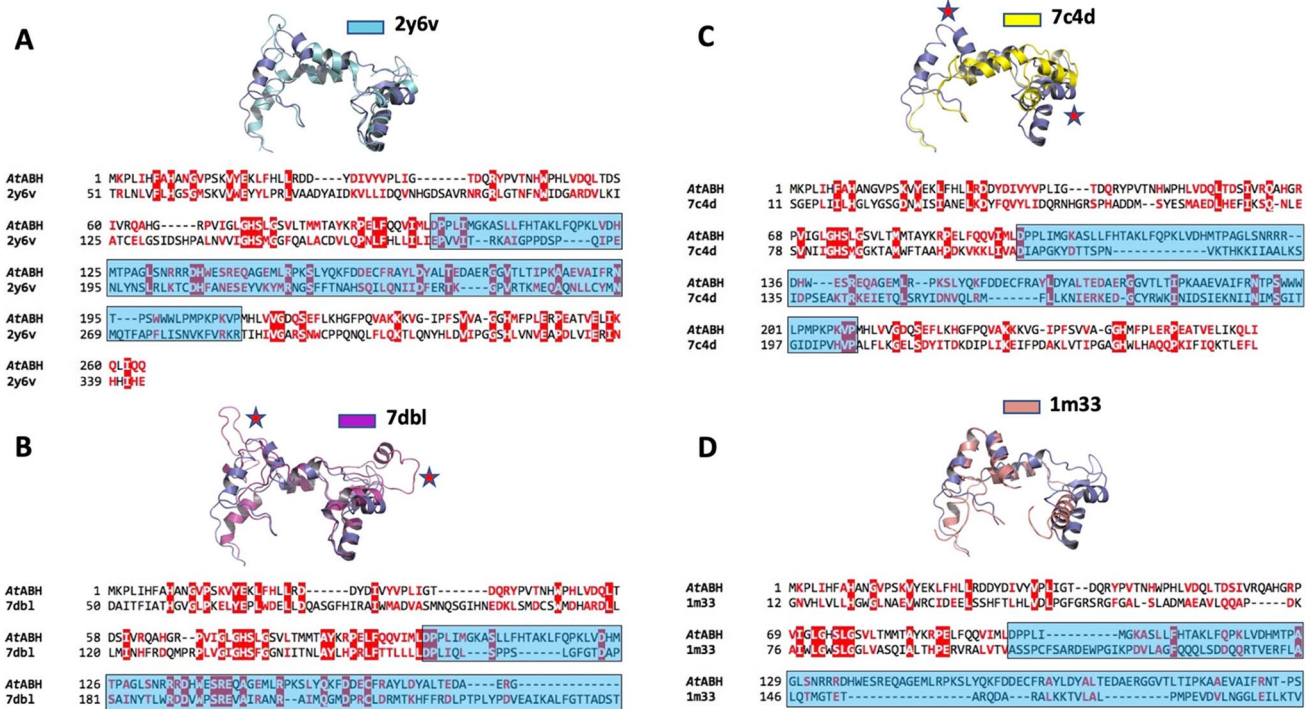


Fig. 5 Analysis of the structural similarity between the cap domains of *AtABH* and its close homologs as determined with DALI. The cap domains of the α B hydrolase Lpx1 from *Saccharomyces cerevisiae* (cyan ribbon model, A; PDB entry: 2y6v), the acyl-CoA hydrolase MpaH from *Penicillium brevicompactum* (magenta ribbon model, B; PDB entry: 7dbl), the marine esterase EprEst (yellow ribbon model, C; PDB entry: 7c4d), and the carboxylesterase BioH from *E. coli*

(orange ribbon model, D; PDB entry: 1m33) are shown superimposed to the cap domain of *AtABH* (blue ribbon model). Structural differences are indicated with a red star. The corresponding structure-based sequence alignment is shown for each structural superposition. Conserved amino acids are shown with white, bold characters and red background and similar residues as red, bold characters

myristate (C14) and *p*-NP palmitate (C16), long-chain, water-insoluble esters. Therefore, *AtABH* behaves as an esterase since it hydrolysed monomeric, water-soluble esters and as a lipase since hydrolysed aggregated, water-insoluble esters (Fojan et al. 2000).

Discussion

A great variety of microorganisms have been reported to be able to transform OTA (Wang et al. 2022), among others some *Acinetobacter* species such as two strains from the *Acinetobacter calcoaceticus* species, namely, *A. calcoaceticus*

NRL B551 and *A. calcoaceticus* 396.1 (De Bellis et al. 2015; Hwang and Draughon 1994) and also the strain *Acinetobacter sp. neg1* (De Bellis et al. 2015), that shows the closest match to *A. gyllenbergii* (Fanelli et al. 2015). Regarding *A. calcoaceticus* NRRL B-551, previous studies revealed that it did not grow in minimal-salts medium containing OTA, indicating that this strain was unable to use OTA as a sole carbon source (Hwang and Draughon 1994). However, when ethanol was added to the minimal-salts medium to provide a carbon source, it was able to grow and degrade OTA at 0.1 $\mu\text{g/mL/h}$ at 30 °C (Hwang and Draughon 1994). Similarly, when peptone was used as the carbon source in the minimal-salts medium, *A. calcoaceticus* 396.1 and

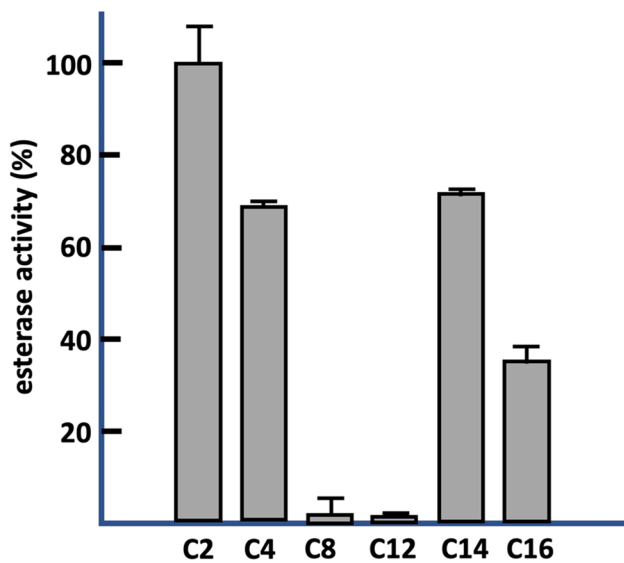


Fig. 6 Substrate profile of *A. tandoii* ABH esterase activity on chromogenic substrates (*p*-nitrophenyl esters) with different acyl chain lengths (C2, acetate; C4, butyrate; C8, caprylate; C12, laurate; C14, myristate; C16, palmitate). The figure shows the relative specificities obtained toward different substrates. The error bars represent the standard deviation estimated from the three independent assays. The observed maximum activity was defined as 100%

Acinetobacter sp. nov. strains also degrade OTA in aerobic conditions and at moderate temperatures (De Bellis et al. 2015). Since these OTA-transforming *Acinetobacter* species are related to clinical environments, in this work we focused our attention on the non-pathogenic strain *A. tandoii* DSM 14970^T with the aim to evaluate its OTA-degrading capacity. Here we showed that cell-free protein extracts of *A. tandoii* DSM 14970^T were competent in OTA degradation (Fig. 1), in contrast to bacterial cultures, which rendered inconclusive results.

In this sense, previous studies identified the carboxypeptidase PJ15_1540 from the *Acinetobacter* sp. *neg1* strain as an enzyme exhibiting hydrolytic activity against OTA. Although the recombinant variant of PJ15_1540 produced in *E. coli* BL21 (DE3) cells hydrolysed OTA, it was poorly efficient since it degraded a low percentage of the OTA present in the cell lysate (Liuzzi et al. 2017); in fact, the activity of this enzyme was much lower than that of the host strain. In this sense, PJ15_1540 is annotated as a D-alanyl-D-alanine carboxypeptidase and therefore potentially involved in the synthesis and remodelling of the peptidoglycan (Egan et al. 2020). In agreement with this, it has a signal peptide (residues Met1-Ala19), and the prediction of its structure with AlphaFold2 (Jumper et al. 2021) reveals an architecture based on an N-terminal D,D-carboxypeptidase domain, and an elongated C-terminal region (Fig. S4 in the Supplementary information), typical of penicillin-binding proteins (PBPs). In fact, the most structurally similar proteins are

PBPs (Table S1 in the Supplementary information). A distinct characteristic of the proposed structure for PJ15_1540 is the presence of a large, amphipathic C-terminal helix (Fig. S4 in the Supplementary information), a structural motif involved in the association of PBPs with the membrane. We consider that this characteristic could make PJ15_1540 and other similar carboxypeptidases sub-optimal enzymes for biotechnological applications aimed at the degradation of OTA since it compromises their solubility. In fact, we think that the presence of this motif may explain the much lower OTA-degrading activity observed for recombinant PJ15_1540 versus the host strain (Liuzzi et al. 2017).

Likewise, similar carboxypeptidases from other sources such as *Bacillus amyloliquefaciens* ASAG1 (Chang et al. 2015), *Bacillus subtilis* CW14 (Hu et al. 2018; Xu et al. 2021), and *Lysobacter* sp. CW239 (Wei et al. 2020) also exhibited a low OTA-degrading activity. Conversely, the presence of OTA-degrading activity in a cp4 carboxypeptidase knock-out *Lysobacter* sp. CW239 strain (Qian et al. 2021) as well as in an amidohydrolase NA deficient *Stenotrophomonas* sp. CW117 strain (Chen et al. 2022) suggests that some strains could contain multiple enzymes for OTA degradation. In agreement with this idea, proteins possessing amidohydrolase (Chen et al. 2022; Dobritsch et al. 2014; Luo et al. 2022; Zhang et al. 2019) or carboxypeptidase activity (Chang et al. 2015; Hu et al. 2018; Liuzzi et al. 2017; Wei et al. 2020; Xu et al. 2022) have been described elsewhere to be able to hydrolyse the amide bond present in the OTA molecule.

Although *A. tandoii* DSM 14970^T possesses a close homolog of the carboxypeptidase PJ15_1540 from the *Acinetobacter* sp. *neg1* strain (Q340_RS0101740), that may contribute to the observed OTA hydrolysis exhibited by protein cell extracts of *A. tandoii* DSM 14970^T, we identified AtABH as an α/β hydrolase that hydrolyses OTA (Fig. 2).

The predicted structure of AtABH (Fig. 4) shows that it belongs to the α/β hydrolase superfamily of enzymes (Heikinheimo et al. 1999; Nardini and Dijkstra 1999; Ollis et al. 1992). The members of this superfamily exhibit an inner structural core based on an eight-stranded mostly parallel β -sheet surrounded on both sides by α -helices, which is decorated with additional structural elements. Typically, one such additional element is an insertion, highly variable both in size and in structure, between canonical β 6 and β 7 strands (β 4 and β 5 in AtABH) that configures the so-called cap domain (Alvarez et al. 2014; Bauer et al. 2020), and that together with other connecting loops between β -strands of the central β -sheet, is key in modulating the entrance of substrates into the binding site of the enzyme. In this regard, the observed hydrolytic activity of AtABH against OTA, OTB, and 4MF reveals that the conformation and dynamics of this cap domain are compatible with the binding of these substrates. Considering this point, we raised the hypothesis that

searching for α/β hydrolases with cap domains similar to that of *AtABH* maybe a good starting point for a roadmap aimed at finding novel OTA-degrading enzymes.

The molecular docking studies with OTA, OTB, and 4MF provide a consistent binding mode common to the three substrates. This binding reveals the presence of two hydrophobic sub-pockets around the catalytic triad of *AtABH*. This result explains well the specificity profile of the enzyme. This latter specificity can be explained assuming that each end of the substrates (N- and C-terminal) binds to a hydrophobic sub-pocket, with their amide bond being located in close proximity to the nucleophile Ser75. Efficient binding would result from a balance between the binding of each end of the substrate to a hydrophobic sub-pocket and the structure of the internal bridge of the molecule between the N- and C-terminal ends. These requirements would not be satisfied by ZA which lacks an internal bridge and a C-terminal large hydrophobic or aromatic residue, HR which has a C-terminal large cationic residue, and ZIF that most probably does not satisfy steric requirements around the nucleophile due to the internal, rigid aliphatic side chain of an Ile residue (Fig. 3). As a whole, these structural results support the binding of the mycotoxins and carboxypeptidase substrates, and in particular, reveal that the conformation of the cap domain permits these substrates to get access into the binding pocket of *AtABH* that is configured by two hydrophobic sub-pockets. Interestingly, the structure of this cap domain is similar to the one from the esterase EprEst (PDB entry: 7c4d; see Table 1) as deduced from structural similarity searches (Fig. 5). This finding is somehow supported by the unexpected esterase activity of *AtABH* and in particular its dependence on the *p*-NP ester chain length that clearly paralleled the one observed for EprEst (Zhu et al. 2021).

These functional results revealing that *AtABH* has both amidohydrolase and esterase activities, indicate that *AtABH* is a promiscuous enzyme (Aharoni et al. 2005; Hult and Berglund 2007; Kourist et al. 2008), which is a relatively common characteristic of members from the $\alpha\beta$ hydrolase superfamily most probably supported by the high versatility of the catalytic triad as catalytic machinery (Kourist et al. 2008; Rauwerdink and Kazlauskas 2015). In this sense, taking into account the time scales of the amidohydrolase and esterase reactions, and in the absence of kinetic analyses, it can be claimed that *AtABH* is operatively much more efficient as esterase than amidohydrolase, in agreement with the observation that promiscuous enzymes exhibit a main, native activity and a second much less efficient one (Aharoni et al. 2005). Thus, we can consider *AtABH* as an esterase with an ancillary amidohydrolase activity.

In summary, our biochemical and structural results indicate that *AtABH* is a promiscuous $\alpha\beta$ hydrolase with a primary esterase activity and a secondary, less efficient

amidohydrolase activity that endows *AtABH* with OTA-degrading capacity. The predicted substrate-binding pocket of *AtABH* reveals two hydrophobic sub-pockets around the nucleophile Ser75, which explains its specificity profile. Also, the prediction of the structure of the carboxypeptidase PJ15_1540 from *Acinetobacter sp. negl* reveals a C-terminal amphipathic α -helix, most probably involved in the association with the membrane, which may explain previous results reporting low activity. Finally, we propose the following procedure for preparing OTA-degrading enzymes: (i) identification of promiscuous $\alpha\beta$ hydrolases with OTA-degrading activity; (ii) prediction of their structures with AlphaFold2, followed by molecular docking studies to determine a plausible OTA-binding mode; (iii) identification and selection of proteins with similar cap domains and substrate-binding pockets; (iv) optimization of OTA-degrading activity through structure-guided preparation of protein variants.

Supplementary Information The online version contains supplementary material available at <https://doi.org/10.1007/s00253-024-13073-x>.

Author contribution R.M., and A.S.A. designed the experiment. A.S.A., C.A.M., and L.P.V. performed the experiments. J.M.M. performed the structural analysis. R.M., A.S.A., J.M.M., B.R., and L.P.V prepared the manuscript. All authors contribute to data analysis.

Funding Open Access funding provided thanks to the CRUE-CSIC agreement with Springer Nature. This work was financially supported by grant PID-2021-123291OB-I00 funded by MCIN/AEI/<https://doi.org/10.13039/501100011033> and by ERDF A Way of Making Europe. Ana Sánchez Arroyo is a recipient of the PRE2018-083862 FPI contract funded by MCIN/AEI/<https://doi.org/10.13039/501100011033> and by ESF Investing in Your Future.

Data availability The authors declare that the data supporting the results of this study are available within the paper and its Supplementary information. Should any raw data be needed, they are available from the corresponding author upon reasonable request.

Declarations

Ethics approval This article does not contain any studies with human participants or animals performed by any of the authors.

Consent for publication All the authors agreed for publication.

Conflict of interest The authors declare no competing interests.

Open Access This article is licensed under a Creative Commons Attribution 4.0 International License, which permits use, sharing, adaptation, distribution and reproduction in any medium or format, as long as you give appropriate credit to the original author(s) and the source, provide a link to the Creative Commons licence, and indicate if changes were made. The images or other third party material in this article are included in the article's Creative Commons licence, unless indicated otherwise in a credit line to the material. If material is not included in the article's Creative Commons licence and your intended use is not permitted by statutory regulation or exceeds the permitted use, you will need to obtain permission directly from the copyright holder. To view a copy of this licence, visit <http://creativecommons.org/licenses/by/4.0/>.

References

- Abraham N, Chan ETS, Zhou T, Seah SYK (2022) Microbial detoxification of mycotoxins in food. *Front Microbiol* 13:1–18. <https://doi.org/10.3389/fmicb.2022.957148>
- Ackerley DF, Gonzalez CF, Park CH, Blake R, Keyhan M, Matin A (2004) Chromate-reducing properties of soluble flavoproteins from *Pseudomonas putida* and *Escherichia coli*. *Appl Environ Microbiol* 70:873–882. <https://doi.org/10.1128/AEM.70.2.873-882.2004>
- Aharoni A, Gaidukov L, Khersonsky O, Gould SMQ, Roodveldt C, Tawfik DS (2005) The “evolvability” of promiscuous protein functions. *Nat Genet* 37:73–76. <https://doi.org/10.1038/ng1482>
- Almagro Armenteros JJ, Tsirigos KD, Sønderby CK, Petersen TN, Winther O, Brunak S, von Heijne G, Nielsen H (2019) SignalP 5.0 improves signal peptide predictions using deep neural networks. *Nat Biotechnol* 37:420–423. <https://doi.org/10.1038/s41587-019-0036-z>
- Alvarez Y, Esteban-Torres M, Cortés-Cabrera A, Gago F, Acebrón I, Benavente R, Mardo K, De Las Rivas B, Muñoz R, Mancheño JM (2014) Esterase LpEst1 from *Lactobacillus plantarum*: a novel and atypical member of the $\alpha\beta$ hydrolase superfamily of enzymes. *PLoS One* 9:e92257. <https://doi.org/10.1371/journal.pone.0092257>
- Amézqueta S, González-Peñas E, Murillo-Arbizu M, López de Cerain A (2009) Ochratoxin A decontamination: a review. *Food Control* 20:326–333. <https://doi.org/10.1016/j.foodcont.2008.05.017>
- Bauer TL, Buchholz PCF, Pleiss J (2020) The modular structure of $\alpha\beta$ -hydrolases. *FEBS J* 287:1035–1053. <https://doi.org/10.1111/febs.15071>
- Blossom DB, Srinivasan A (2008) Drug-resistant *Acinetobacter baumannii-calcoaceticus* Complex. *Inf Dis Clin Pr* 16:1–3
- Carr EL, Kämpfer P, Patel BKC, Gürtler V, Seviour RJ (2003) Seven novel species of *Acinetobacter* isolated from activated sludge. *Int J Syst Evol Microbiol* 53:953–963. <https://doi.org/10.1099/ijs.0.02486-0>
- Chang X, Wu Z, Wu S, Dai Y, Sun C (2015) Degradation of ochratoxin A by *Bacillus amyloliquefaciens* ASAG1. *Food Addit Contam - Part A Chem Anal Control Expo Risk Assess* 32:564–571. <https://doi.org/10.1080/19440049.2014.991948>
- Chen N, Fei Q, Luo H, Fang Z, Xiao Y, Du Z, Yu Z (2022) Isoenzyme N -Acyl-L-amino acid amidohydrolase NA increases ochratoxin A degradation efficacy of *Stenotrophomonas sp.* CW117 by enhancing amidohydrolase ADH3 stability. *Microbiol Spectr* 10:e02205-e2222
- Claeys L, Romano C, De Ruyck K, Wilson H, Fervers B, Korenjak M, Zavadil J, Gunter MJ, De Saeger S, De Boevre M, Huybrechts I (2020) Mycotoxin exposure and human cancer risk: a systematic review of epidemiological studies. *Compr Rev Food Sci Food Saf* 19:1449–1464. <https://doi.org/10.1111/1541-4337.12567>
- Curiel JA, De Las RB, Mancheño JM, Muñoz R (2011) The pURI family of expression vectors: a versatile set of ligation independent cloning plasmids for producing recombinant His-fusion proteins. *Protein Expr Purif* 76:44–53. <https://doi.org/10.1016/j.pep.2010.10.013>
- De Bellis P, Tristezza M, Haidukowski M, Fanelli F, Sisto A, Mulè G, Grieco F (2015) Biodegradation of ochratoxin a by bacterial strains isolated from vineyard soils. *Toxins (basel)* 7:5079–5093. <https://doi.org/10.3390/toxins7124864>
- Del Prete V, Rodriguez H, Carrascosa AV, De Las RB, Garcia-Moruno E, Muñoz R (2007) In vitro removal of ochratoxin A by wine lactic acid bacteria. *J Food Prot* 70:2155–2160. <https://doi.org/10.4315/0362-028X-70.9.2155>
- Schrödinger L, DeLano WL (2020) PyMOL. Available at: <http://www.pymol.org/pymol>
- Dobritzsch D, Wang H, Schneider G, Yu S (2014) Structural and functional characterization of ochratoxinase, a novel mycotoxin-degrading enzyme. *Biochem J* 462:441–452. <https://doi.org/10.1042/BJ20140382>
- Egan AJF, Errington J, Vollmer W (2020) Regulation of peptidoglycan synthesis and remodelling. *Nat Rev Microbiol* 18:446–460. <https://doi.org/10.1038/s41579-020-0366-3>
- Emsley P, Lohkamp B, Scott WG, Cowtan K (2010) Features and development of Coot. *Acta Crystallogr Sect D Biol Crystallogr* 66:486–501. <https://doi.org/10.1107/S0907444910007493>
- Esteban-Torres M, Reverón I, Mancheño JM, De las Rivas B, Muñoz R (2013) Characterization of a feruloyl esterase from *Lactobacillus plantarum*. *Appl Environ Microbiol* 79:5130–5136. <https://doi.org/10.1128/AEM.01523-13>
- Fanelli F, Chiara M, Liuzzi VC, Haidukowski M, Tristezza M, Caterina M, D’Erchia AM, Pesole G, Horner DS, Mule G (2015) Draft genome sequence of *Acinetobacter sp. neg1* capable of degrading ochratoxin A. *FEMS Microbiol Lett* 362:1–4. <https://doi.org/10.1093/femsle/fnv004>
- Fojan P, Jonson PH, Petersen MTN, Petersen SB (2000) What distinguishes an esterase from a lipase: a novel structural approach. *Biochimie* 82:1033–1041. [https://doi.org/10.1016/S0300-9084\(00\)01188-3](https://doi.org/10.1016/S0300-9084(00)01188-3)
- Forli S, Huey R, Pique ME, Sanner MF, Goodsell DS, Olson AJ (2016) Computational protein-ligand docking and virtual drug screening with the AutoDock suite. *Nat Protoc* 11:905–919. <https://doi.org/10.1038/nprot.2016.051>
- Gan F, Zhou Y, Hou L, Qian G, Chen X, Huang K (2017) Ochratoxin A induces nephrotoxicity and immunotoxicity through different MAPK signaling pathways in PK15 cells and porcine primary splenocytes. *Chemosphere* 182:630–637. <https://doi.org/10.1016/j.chemosphere.2017.05.030>
- Heikinheimo P, Goldman A, Jeffries C, Ollis DL (1999) Of barn owls and bankers: a lush variety of $\alpha\beta$ hydrolases. *Structure* 7:141–146. [https://doi.org/10.1016/S0969-2126\(99\)80079-3](https://doi.org/10.1016/S0969-2126(99)80079-3)
- Holm L (2022) Dali server : structural unification of protein families. *Nucleic Acids Res* 50:W210–W215
- Hu HN, Jia X, Wang YP, Liang ZH (2018) Removal of ochratoxin A by a carboxypeptidase and peptides present in liquid cultures of *Bacillus subtilis* CW14. *World Mycotoxin J* 11:559–570. <https://doi.org/10.3920/WMJ2017.2296>
- Hult K, Berglund P (2007) Enzyme promiscuity: mechanism and applications. *Trends Biotechnol* 25:231–238. <https://doi.org/10.1016/j.tibtech.2007.03.002>
- Hwang C-A, Draughon FA (1994) Degradation of ochratoxin A by *Acinetobacter calcoaceticus*. *J Food Prot* 57:410–414. <https://doi.org/10.4315/0362-028x-57.5.410>
- Jumper J, Evans R, Pritzel A, Green T, Figurnov M, Ronneberger O, Tunyasuvunakool K, Bates R, Židek A, Potapenko A, Bridgland A, Meyer C, Kohl SAA, Ballard AJ, Cowie A, Romera-Paredes B, Nikolov S, Jain R, Adler J, Back T, Petersen S, Reiman D, Clancy E, Zielinski M, Steinegger M, Pacholska M, Berghammer T, Bodenstein S, Silver D, Vinyals O, Senior AW, Kavukcuoglu K, Kohli P, Hassabis D (2021) Highly accurate protein structure prediction with AlphaFold. *Nature* 596:583–589. <https://doi.org/10.1038/s41586-021-03819-2>
- Jung J, Park W (2015) *Acinetobacter* species as model microorganisms in environmental microbiology: current state and perspectives. *Appl Microbiol Biotechnol* 99:2533–2548. <https://doi.org/10.1007/s00253-015-6439-y>
- Kourist R, Bartsch S, Fransson L, Hult K, Bornscheuer UT (2008) Understanding promiscuous amidase activity of an esterase

- from *Bacillus subtilis*. *ChemBioChem* 9:67–69. <https://doi.org/10.1002/cbic.200700521>
- Li Z, Jaroszewski L, Iyer M, Sedova M, Godzik A (2020) FATCAT 2.0: towards a better understanding of the structural diversity of proteins. *Nucleic Acids Res* 48:W60–W64. <https://doi.org/10.1093/nar/gkaa443>
- Liebschner D, Afonine PV, Baker ML, Bunkoczi G, Chen VB, Croll TI, Hintze B, Hung L-W, Jain S, McCoy AJ, Moriarty NW, Oeffner RD, Poon BK, Prisant MG, Read RJ, Richardson JS, Richardson DC, Sammito MD, Sobolev OV, Stockwell DH, Terwilliger TC, Urzhumtsev AG, Videau LL, Williams CJ, Adams PD (2019) Macromolecular structure determination using X-rays, neutrons and electrons: recent developments in Phenix. *Acta Crystallogr Sect d, Struct Biol* D75:861–877. <https://doi.org/10.1107/S2059798319011471>
- Liuzzi VC, Fanelli F, Tristezza M, Haidukowski M, Picardi E, Manzari C, Lionetti C, Grieco F, Logrieco AF, Thon MR, Pesole G, Mulè G (2017) Transcriptional analysis of *Acinetobacter sp. neg1* capable of degrading ochratoxin A. *Front Microbiol* 7:1–9. <https://doi.org/10.3389/fmicb.2016.02162>
- Luo H, Wang G, Chen N (2022) A superefficient Ochratoxin A hydrolase with promising potential for industrial applications. *Appl Environ Microbiol* 88:e01964–e2021. <https://doi.org/10.1128/AEM.01964-21>
- Marin S, Ramos AJ, Cano-Sancho G, Sanchis V (2013) Mycotoxins: occurrence, toxicology, and exposure assessment. *Food Chem Toxicol* 60:218–237. <https://doi.org/10.1016/j.fct.2013.07.047>
- McCoy AJ, Sammito MD, Read RJ (2022) Implications of AlphaFold2 for crystallographic phasing by molecular replacement. *Acta Crystallogr Sect d, Struct Biol* 78:1–13. <https://doi.org/10.1107/S2059798321012122>
- Nardini M, Dijkstra BW (1999) α/β hydrolase fold enzymes: the family keeps growing. *Curr Opin Struct Biol* 9:732–737. [https://doi.org/10.1016/S0959-440X\(99\)00037-8](https://doi.org/10.1016/S0959-440X(99)00037-8)
- Ndiaye S, Zhang M, Fall M, Ayessou NM, Zhang Q, Li P (2022) Current review of mycotoxin biodegradation and bioadsorption: microorganisms, mechanisms, and main important applications. *Toxins (Basel)* 14:729. <https://doi.org/10.3390/toxins14110729>
- Nemec A, Musilek M, Maixnerová M, De Baere T, van der Reijden TJK, Vannechoutte M, Dijkshoorn L (2009) *Acinetobacter beijerinckii* sp. nov. and *Acinetobacter gyllenbergii* sp. nov., haemolytic organisms isolated from humans. *Int J Syst Evol Microbiol* 59:118–124. <https://doi.org/10.1099/ijs.0.001230-0>
- Ollis DL, Cheah E, Cygler M, Dijkstra B, Frolov F, Franken SM, Harel M, Remington SJ, Silman I, Schrag J, Sussman JL, Verschuereen KHG, Goldman A (1992) The α/β hydrolase fold. *Protein Eng* 5:197–211
- Pereira J, Simpkin AJ, Hartmann MD, Rigden DJ, Keegan RM, Lupas AN (2021) High-accuracy protein structure prediction in CASP14. *Proteins* 89:1687–1699. <https://doi.org/10.1002/prot.26171>
- Petersen EF, Goddard TD, Huang CC, Couch GS, Greenblatt DM, Meng EC, Ferrin TE (2004) UCSF Chimera - a visualization system for exploratory research and analysis. *J Comput Chem* 25:1605–1612. <https://doi.org/10.1002/jcc.20084>
- Pfohl-Leszkowicz A, Manderville RA (2007) Ochratoxin A: an overview on toxicity and carcinogenicity in animals and humans. *Mol Nutr Food Res* 51:61–99. <https://doi.org/10.1002/mnfr.200600137>
- Qian Y, Zhang X, Fei Q, Zhou Y (2021) Comments on the ochratoxin A degradation mechanism by *Lysobacter* sp CW239 — Wei Wei et al. (2020). *Environ Pollut* 281:117063. <https://doi.org/10.1016/j.envpol.2021.117063>
- Rauwerdink A, Kazlauskas RJ (2015) How the same core catalytic machinery catalyzes 17 different reactions: the Serine-Histidine-Aspartate catalytic triad of alpha/beta-Hydrolase Fold Enzymes. *ACS Catal* 5:6153–6176. <https://doi.org/10.1021/acscatal.5b01539>
- Read RJ, Baker EN, Bond ChS, Garman EF, van Raaij MJ (2023) Alpha-Fold and the future of structural biology. *Acta Crystallogr Sect d, Struct Biol* 79:556–558. <https://doi.org/10.1107/S20597983004928>
- Sánchez-Arroyo A, Plaza-Vinuesa L, Rivas B de las, Mancheño JM, Muñoz R (2023) The salicylate 1,2-dioxygenase from *Pseudaminobacter salicylatoxidans* DSM 6986T is a bifunctional enzyme that inactivates the mycotoxin ochratoxin A by a novel amidohydrolase activity. *Int J Biol Macromol* 237:124230. <https://doi.org/10.1016/j.ijbiomac.2023.124230>
- Shabtai Y, Gutnick DL (1985) Exocellular esterase and emulsan release from the cell surface of *Acinetobacter calcoaceticus*. *J Bacteriol* 161:1176–1181. <https://doi.org/10.1128/jb.161.3.1176-1181.1985>
- Tunyasyunakool K, Adler J, Wu Z, Green T, Zielinski M, Židek A, Bridgland A, Cowie A, Meyer C, Laydon A, Velankar S, Kleywegt GJ, Bateman A, Evans R, Pritzel A, Figurnov M, Ronneberger O, Bates R, Kohl SAA, Potapenko A, Ballard AJ, Romera-Paredes B, Nikolov S, Jain R, Clancy E, Reiman D, Petersen S, Senior AW, Kavukcuoglu K, Birney E, Kohli P, Jumper J, Hassabis D (2021) Highly accurate protein structure prediction for the human proteome. *Nature* 596:590–596. <https://doi.org/10.1038/S41586-021-03828-1>
- Wang L, Hua X, Shi J, Jing N, Ji T, Lv B, Liu L, Chen Y (2022) Ochratoxin A: occurrence and recent advances in detoxification. *Toxicon* 210:11–18. <https://doi.org/10.1016/j.toxicon.2022.02.010>
- Wei W, Qian Y, Wu Y, Chen Y, Peng C, Luo M, Xu J, Zhou Y (2020) Detoxification of ochratoxin A by *Lysobacter* sp. CW239 and characteristics of a novel degrading gene carboxypeptidase cp4. *Environ Pollut* 258:113677. <https://doi.org/10.1016/j.envpol.2019.113677>
- Williams CJ, Headd JJ, Moriarty NW, Prisant MG, Videau LL, Deis LN, Verma V, Keedy DA, Hintze BJ, Chen VB, Jain S, Lewis SM, Arendall WB, Snoeyink J, Adams PD, Lovell SC, Richardson JS, Richardson DC (2018) MolProbity: more and better reference data for improved all-atom structure validation. *Protein Sci* 27:293–315. <https://doi.org/10.1002/pro.3330>
- Xu H, Wang L, Sun J, Wang L, Guo H, Ye Y, Sun X (2022) Microbial detoxification of mycotoxins in food and feed. *Crit Rev Food Sci Nutr* 62:4951–4969. <https://doi.org/10.1080/10408398.2021.1879730>
- Xu X, Pang M, Liu J, Wang Y, Wu X, Huang KL, Liang Z (2021) Genome mining reveals the genes of carboxypeptidase for OTA-detoxification in *Bacillus subtilis* CW14. *Int J Biol Macromol* 186:800–810. <https://doi.org/10.1016/j.ijbiomac.2021.07.085>
- Yoon EJ, Goussard S, Nemec A, Lambert T, Courvalin P, Grillot-Courvalin C (2016) Origin in *Acinetobacter gyllenbergii* and dissemination of aminoglycoside-modifying enzyme AAC(6′)-Ih. *J Antimicrob Chemother* 71:601–606. <https://doi.org/10.1093/jac/dkv390>
- Zarrilli R, Visca P, Bonnin RA, Dé E (2023) Editorial: drug resistance, global epidemiology and virulence of *Acinetobacter*. *Front Microbiol* 14:28–30. <https://doi.org/10.3389/fmicb.2023.1151462>
- Zhang H, Zhang Y, Yin T, Wang J, Zhang X (2019) Heterologous expression and characterization of a novel Ochratoxin A degrading enzyme, N-acyl-L-amino acid amidohydrolase, from *Alcaligenes faecalis*. *Toxins (basel)* 11:1–8. <https://doi.org/10.3390/toxins11090518>
- Zhu C, Chen Y, Isupov MN, Littlechild JA, Sun L, Liu X, Wang Q, Gong H, Dong P, Zhang N, Wu Y (2021) Structural insights into a novel esterase from the East Pacific rise and its improved thermostability by a semirational design. *J Agric Food Chem*. <https://doi.org/10.1021/acs.jafc.0c06338>

Publisher's Note Springer Nature remains neutral with regard to jurisdictional claims in published maps and institutional affiliations.